SERI/TP-213-2689
UC Category: 63
DE85012166

Structural and Electrical Characterization of Polycrystalline Semiconductor Materials

Richard J. Matson
Y. Simon Tsuo

July 1985

Prepared for the
1985 Spring Meeting of the
Materials Research Society
San Francisco, California
15-18 April 1985

Prepared under Task No. 3411.10
FTP No. 460

Solar Energy Research Institute
A Division of Midwest Research Institute

1617 Cole Boulevard
Golden, Colorado 80401

Prepared for the
U.S. Department of Energy
Contract No. DE-AC02-83CH10093

Printed in the United States of America
Available from:
National Technical Information Service
U.S. Department of Commerce
5285 Port Royal Road
Springfield, VA 22161

Price: Microfiche A01
Printed Copy A02

Codes are used for pricing all publications. The code is determined by the number of pages in the publication. Information pertaining to the pricing codes can be found in the current issue of the following publications, which are generally available in most libraries: *Energy Research Abstracts, (ERA); Government Reports Announcements* and Index (*GRA* and I); *Scientific and Technical Abstract Reports (STAR);* and publication, NTIS-PR-360 available from NTIS at the above address.

STRUCTURAL AND ELECTRICAL CHARACTERIZATION OF POLYCRYSTALLINE SEMICONDUCTOR MATERIALS

Richard J. Matson and Y. Simon Tsuo
Solar Energy Research Institute
Golden, Colorado 80401 USA

ABSTRACT

Secondary electron imaging, electron channeling and electron-beam-induced current (EBIC) are used alternately in a scanning electron microscope to characterize and correlate the morphology, crystallographic orientation, and electronic quality (types and spatial distribution of defects) of individual grains in polycrystalline semiconductor samples. The technique is discussed in some detail, and a number of applications and results in the study of edge-supported-pulling (ESP) silicon sheet and low-angle silicon sheet (LASS) materials are reported.

INTRODUCTION

A considerable amount of research is being conducted on low-cost polycrystalline semiconductors in the photovoltaic industry. The grain sizes of these polycrystalline materials are on the order of millimeters or less, and the electronic quality of individual grains is often related to their crystallographic orientations and intragrain defect structure. Secondary electron imaging (SEI), electron channeling (EC), and electron-beam-induced current (EBIC) techniques using the scanning electron microscope (SEM) have been combined to determine and correlate the morphology, the crystallographic orientations, and the electronic quality of individual grains in polycrystalline semiconductor samples. EBIC can also be used to determine the minority carrier diffusion length of individual grains and the effective minority carrier recombination rate at the grain boundaries. These techniques have been used to study two promising silicon sheet growth techniques, edge-supported-pulling (ESP) silicon sheet and low-angle silicon sheet (LASS). The techniques themselves, their applications to these materials, and the experimental results are discussed.

EXPERIMENTAL METHODS

Electron-beam-induced current microscopy is also known as charge-collection scanning microscopy [1]. The EBIC image results from the electron-hole pairs, or current, created by the electron beam and separated by the semiconductor junction field [2]. This current collection will change in the presence of electrically active defects, or recombination centers, where the EBIC signal decreases. This results in either a dip in the EBIC linescan or a darkening in the intensity-modulated EBIC map. Figure 1 illustrates the effect of a grain boundary on an EBIC linescan. The

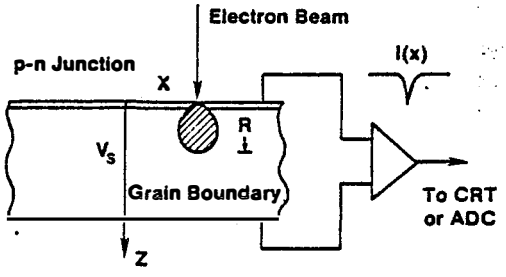

Fig. 1. Schematic illustration of the EBIC imaging of a grain boundary in a polycrystalline solar cell. (After C. Donolato and R. Bell)

amplified EBIC signal can be used to modulate the intensity of the SEM CRT to create a map, or image, of electrically active defects. In planar EBIC, or EBIC performed with the beam normal to the junction as shown in Figure 1, the EBIC map (Figure 2a) can be compared with the corresponding SEI (Figure 2b) to correlate topographical features such as the grain boundaries and twin planes, and their effect on device performance. Figure 2 shows such a comparison for a metal oxide semiconductor (MOS) structure made from Wacker cast polycrystalline silicon [3]. As can be seen, the density of defects can be measured from EBIC maps. EBIC linescans and other EBIC techniques can be used to measure minority carrier diffusion lengths of individual grains [3,4]. EBIC linescans can also be used to measure the effective recombination rate at grain boundaries [3,5]. These kinds of analyses can also be easily automated [6]. In junction EBIC, or EBIC performed parallel to a cleaved junction, a comparison of SEI and EBIC can be used to locate the electrical junction with respect to the physical geometry of the structure [7].

Electron channeling (EC) with our instrument, a JEOL 35C, consists of rocking a collimated beam of electrons about a fixed point and recording the pattern of secondary, absorbed, or backscattered electrons. Figure 3 illustrates a particle beam model for the variation in electron backscattering as the incident beam changes its angle relative to the crystal lattice. When the beam is traveling parallel to a set of planes, backscattering is reduced [8]. The usual method of determining a sample's crystallographic orientation and structure is to compare its ECP with a unit stereographic triangle of the same structure [8].

The three imaging modes (SEI, EBIC, and EC) can be used alternately on the same sample location by means of a modified integrated circuit SEM EBIC stage, which has been discussed elsewhere [7]. A discussion of several different applications for the complementary use of these techniques follows.

Fig. 2. A comparison of the EBIC image (a) and the SEI (b) of a polycrystalline MOS device.

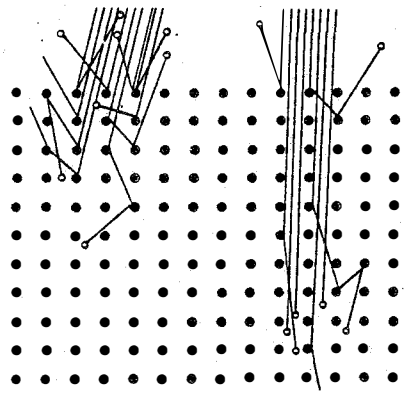

Fig. 3. A particle model for the variation in electron backscattering as the incident beam changes its angle relative to a crystal lattice. This variation results in the observed ECP.

STUDY OF EDGE-SUPPORTED-PULLING SILICON SHEETS

Developed at the Solar Energy Research Institute (SERI), the edge-supported pulling (ESP) process involves the formation of a capillary film of liquid Si between two parallel filaments (4 cm apart) immersed in molten silicon. As the filaments are pulled away from the melt, the remote region of the film solidifies between the filaments in a continuous fashion while the meniscus is replenished by capillarity (Figure 4). This process results in large, longitudinal grains that dominate the silicon sheet, while a fine grain structure is characteristic of the first few millimeters closest to the filaments [9].

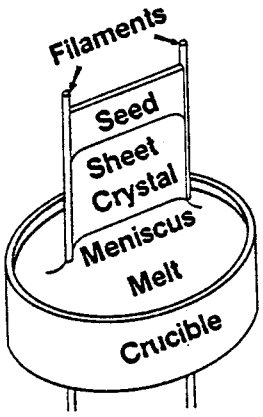

Fig. 4. Diagram of the ESP process showing a capillary film of liquid silicon forming between two parallel filaments as the filaments are pulled through the molten silicon.

Electron channeling patterns were recorded for grains wider than about 0.5 mm for three different sample growth conditions (Figure 5). The orientations of the surface normal of the individual grains (dots) and their respective grain growth direction during ribbon pulling (arrows) were plotted on a stereographic projection unit triangle. The different growth conditions resulted in three different sheet thicknesses: (a) 1100 μm, (b) 480 μm, and (c) 100 μm. This analysis demonstrated that the thinner sheet resulting from higher melt temperatures and/ or faster pulling speeds corresponded to a more coherent structure among the grains, which showed a preference for surface normals of [011] and a grain growth direction along the (111) plane [10].

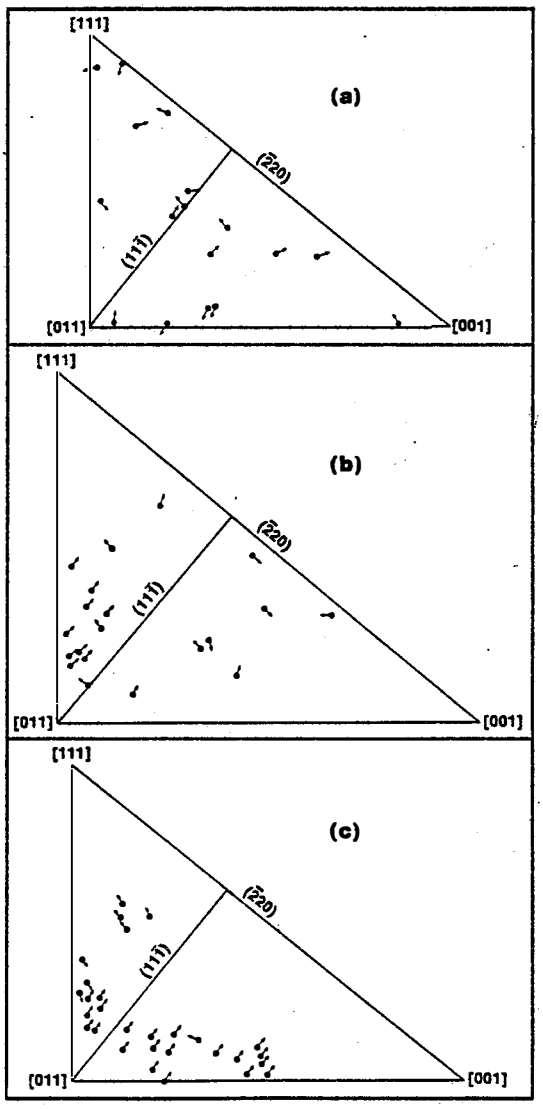

Fig. 5. Grain orientations of ESP sheets, for average sheet thicknesses of (a) 110 μm, (b) 480 μm, and (c) 110 μm.

After a Schottky barrier to the material was formed, EBIC maps of each sample were recorded. The map of the 480-μm-thick sample is shown in Figure 6. The variation in the intensity of the EBIC signal between grains corresponds to the varying densities of electrically active dislocations. These ranged from $5 \cdot 10^3$ cm^{-2} to $2 \cdot 10^5 cm^{-2}$. An EBIC linescan across these grains shows that the average variation in the short-circuit current, and therefore in the energy conversion efficiency, from the light grains to the dark grains is about 20% [10]. Digital EBIC linescans across the boundary between the metallized or Schottky barrier portion of the sample and the bulk for the indi-

vidual grains were recorded to measure the diffusion length of each grain. Dislocation densities were also measured from more highly magnified EBIC maps of the grains. The result was a clear correlation between the defect density, the diffusion length, and the short-circuit current of the grains.

A comparison of the ECP and the EBIC analyses revealed that the high-current grains all had surface orientations near the [011]. This result is consistent with the fact that the largest grain sizes and the highest-efficiency solar cells to date from ESP silicon sheets were achieved using seeds with the [011] surface normal and having (111) twin planes parallel to the filaments to block the propagation of spurious grains.

These analyses were extended to studies of the hydrogen passivation of ESP materials [11]. Samples, partially masked during hydrogen ion bombardment, were analyzed with EBIC maps and linescans and electron channeling. Figure 7 shows a typical EBIC result. The EBIC linescans show the effect of the material's passivation relative to the same baseline, or zero beam current line, at the bottom of the figure. Because of the differential amplification of the EBIC signal, the EBIC maps do not necessarily indicate the true relative effect. A comparison of the degree, or extent, of passivation of the grain boundaries and intragrain defects with the adjacent grain orientation mismatch and the individual grain orientations, respectively, did not show any clear correlation. The grain boundary result is to be expected, because an ECP characterizes only three of the five degrees of freedom possible for a grain boundary.

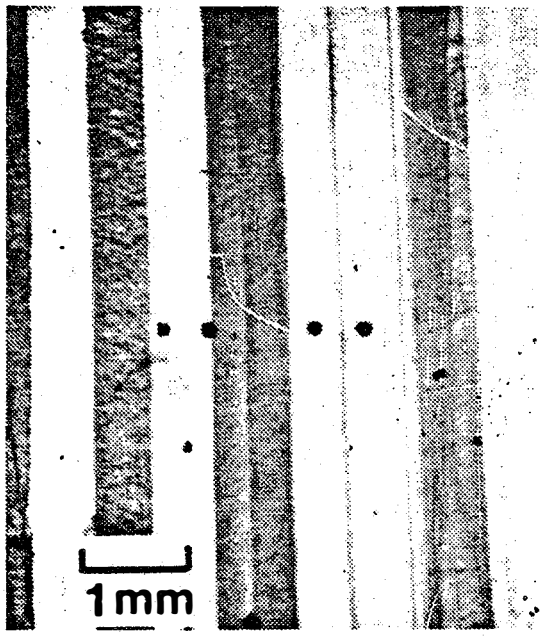

Fig. 6. The EBIC image of an area of the 480-μm-thick sample.

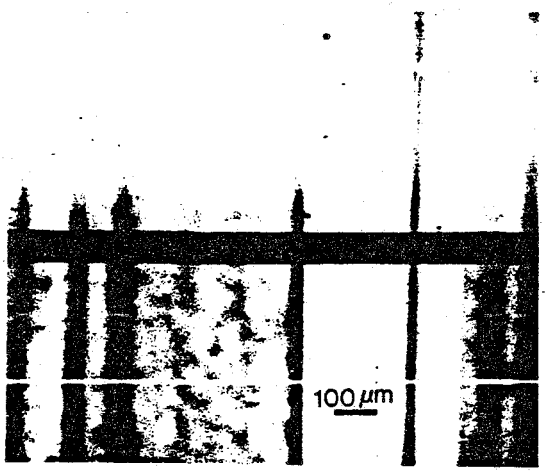

Fig. 7. The EBIC image of a sample with areas with and without hydrogen passivation. The EBIC linescans are taken from the two different areas and show the passivation effect most clearly.

STUDY OF LOW-ANGLE SILICON SHEET

The low-angle silicon sheet (LASS) growth process is a high-throughput silicon sheet growth method developed by the Energy Materials Corporation of South Lancaster, Massachusetts. In the LASS growth process, a silicon sheet 5 to 6 cm wide and 0.5 to 1.0 mm thick is pulled almost horizontally from a melt contained in a

shallow, rectangular crucible (Figure 8). The solidus-liquidus interface area of this process is significantly greater than those of vertical silicon sheet pulling processes, such as the dendritic web and ESP methods. The efficient extraction of the latent heat of fusion in the LASS process makes very high linear growth rates possible--typically, 30 to 40 cm/min.

Recently, conditions have been found that occasionally foster the growth of large areas of twin-stabilized, planar growth LASS material at a speed of about 200 cm^3/min. These areas were essentially single crystalline, which was determined by close observation of the ECPs produced while moving the electron beam across the surface of an as-grown sample. The as-grown surface is topographically quite variable, which is seen in both random and parallel dendritic growths that may extend as high as 0.5 mm from the surface [12]. The crystallinity of these large areas was further confirmed by polishing the sample and performing preferential etch and EBIC studies on the same material. EC showed the surface normal of this crystalline area to be [111]. A correlation of light micrographs, SEIs, and ECPs of sample top surfaces showed that the parallel, faceted structure of the sample top surface of this twin-stabilized planar growth material runs along the (211) plane [12].

In addition to dislocations and stacking faults, polycrystalline silicon islands (inclusions) and what appear to be large dislocation loops have been observed in the twin-stabilized planar growth material (Figure 9). EC showed that the crystallo-

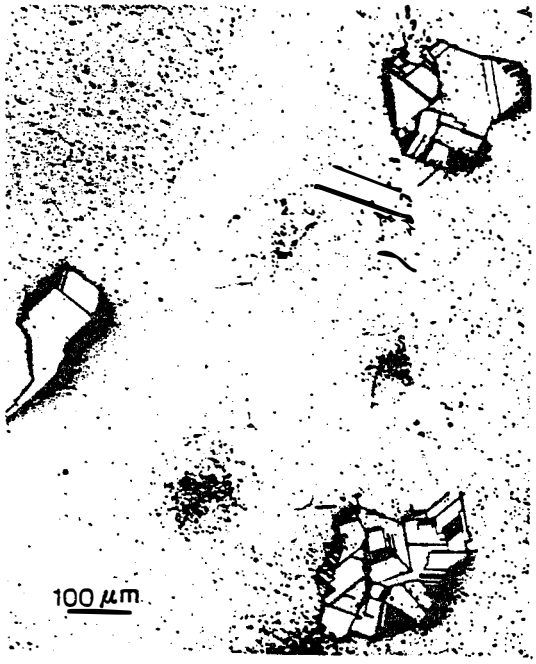

Fig. 9. A light micrograph of an area of twin-stabilized growth in a LASS sample illustrating localized defect structures.

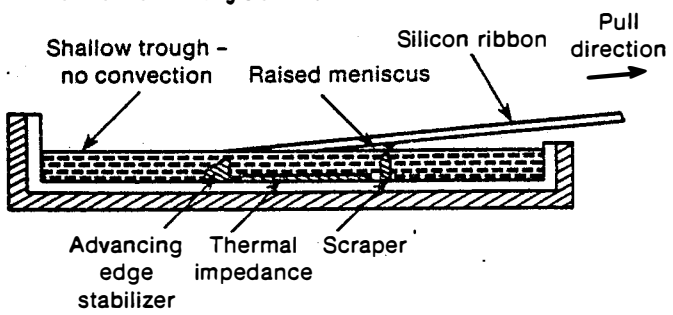

Fig. 8. Diagram of the LASS process. This is similar to the ESP process, except that the sheet is drawn almost horizontally.

graphic orientation of these polycrystalline islands is different from that of the surrounding crystal. The islands do not, however, disrupt the mechansim for the single-crystal growth surrounding them. They result from the entrapment of small droplets of liquid that solidified after the surrounding crystal was formed during sheet growth [12].

An example of large dislocation loops or complexes is shown in Figure 10. The SEI (a) of the dislocation etch pits was later compared with an EBIC micrograph (b) of the same area after the sample was repolished and a diffused p-n junction was formed in the material, to compare the information yielded by the two different techniques. Superimposing the ECP of the central area of this complex with either the SEI in (a) or the EBIC image in (b) in situ shows that the stacking faults occur along the (110) planes. A comparison of the ECP inside and outside this particular defect structure showed the same crystallographic orientation.

Fig. 10. Defect structure in a single-crystal area of a LASS sample: (a) SEI of the area after dislocation etching; (b) EBIC image of the same area after mechanical and chemical polishing; and (c) the superposition of an ECP and the SEI of the center of the defect structure in (a), but at a higher magnification.

CONCLUSIONS

Combining secondary electron imaging, electron channeling, and EBIC techniques in a SEM revealed the dominant grain structure of thin ESP silicon sheets, and such grains tend to have a better electronic quality than randomly oriented grains. This technique was also used to correlate the structural and electrical properties of defects in LASS material. The EBIC and EC results provided important clues to the mechanisms of the nucleation and termination of single-crystal LASS growth. As such, these techniques are quite useful in correlating the structural, electrical, and topographical features of newly emerging polycrystalline semiconductor materials.

ACKNOWLEDGMENTS

We wish to thank T. Ciszek and J. Hurd of SERI, originators of the ESP sheet growth technique, and D. Jewett and J. Milstein of the Energy Materials Corporation for their cooperation and for providing the samples for these studies. This work was supported by the U.S. Department of Energy under contract no. DE-AC02-83CH10093.

REFERENCES

[1] D. B. Holt, in Quantitative Scanning Electron Microscopy, edited by D. B. Holt, M. D. Muir, P. R. Grant, and I. M. Boswarva, (Academic Press, London, 1974), p. 213.
[2] H. J. Leamy, J. Appl. Phys. 53, R51 (1982).
[3] P. E. Russell, Ph.D. thesis, University of Florida, 1982.
[4] W. H. Hacket, Jr.; J. Appl. Phys. 43, 1649 (1972).
[5] D. E. Burk, S. Kanner, J. E. Muyshondt, D. S. Shaulis, and P. E. Russell, J. Appl. Phys. 54, 169 (1983).
[6] P. E. Russell, C. R. Herrington, and R. J. Matson, Technology in Review 1, 3 (1983).
[7] R. J. Matson, Scanning Electron Microscopy/1984 (SEM, Inc., O'Hare, ILL 1984) p. 625.
[8] D. C. Joy, D. E. Newbury, and D. L. Davidson, J. Appl. Phys. 53, R81 (1982).
[9] T. F. Ciszek, Silicon Processing for Photovoltaics, edited by C. P. Khattak and K. V. Ravi (Elsevier Science Publishers, New York, 1985) p. 131.
[10] Y. S. Tsuo, J. L. Hurd, R. J. Matson, and T. F. Ciszek, IEEE-ED ED-31, 614 (1984).
[11] Y. S. Tsuo and J. B. Milstein, Appl. Phys. Lett. 45, 971 (1984).
[12] Y. S. Tsuo, R. J. Matson, J. B. Milstein, and T. W. Schuyler, J. Crystal Growth (in press).